American Journal of Pathology, Vol. 164, No. 6, June 2004

Differential Expression of Splicing Variants of the Human Caldesmon Gene (*CALD1*) in Glioma Neovascularization *versus* Normal Brain Microvasculature

Ping-Pin Zheng,* Anieta M. Sieuwerts,† Theo M. Luider,‡ M. van der Weiden,* Peter A.E. Sillevis-Smitt,‡ and Johan M. Kros*

From the Department of Pathology, Internal Oncology,† Neuro-Oncology and Neurology,‡ Erasmus Medical Center, Rotterdam, The Netherlands*

Caldesmon is a cytoskeleton-associated protein which has not yet been related to neoplastic angiogenesis. In this study we investigated the expression of the caldesmon gene (*CALD1*) splicing variants and the protein expression level in glioma microvessels *versus* normal brain microvasculature. To exclude sources of splice variant expression from non-vascular components all possible cellular components present in control and glioma samples were prescreened by laser-capture microdissection followed by RT-PCR before the cohort study. We discovered differential expression of the splicing variants of *CALD1* in the tumor microvessels in contrast to normal brain microvasculature. Missplicing of exons 1, 1 + 4, and 1′ + 4 of the gene is exclusively found in glioma microvessels. To exclude the possibility that this missplicing results from splice-site mutations, mutation scanning was performed by a coupled *in vitro* transcription/translation assay (IVTT). No premature stop mutations were traced by the IVTT. The transcriptional changes consequently resulted in up-regulation at the protein expression level. The up-regulated expression of caldesmon was coincident with the down-regulated expression of tight junction proteins (occludin and ZO-1). The results support the notion that missplicing of the *CALD1* gene in glioma microvasculature is an independent epigenetic event regulated at the transcriptional level. The event coexists with tight junction (TJ) breakdown of the endothelial cells in glioma microvasculature. The data reveal a novel mechanism contributing to dysfunctionality of glioma neovascularization. *(Am J Pathol 2004, 164:2217–2228)*

Genome-wide analyses have revealed that 40 to 60% of human genes undergo alternative splicing.[1] Alternative splicing, therefore, seems to contribute considerably to enable the highly complex and diverse functions encoded by the human genome. Alternative splicing permits vertebrate pre-mRNA to be processed into multiple mRNAs differing in their precise combination of exon sequences, resulting in the encoding of different protein isoforms.[2] Multiple modes of alternative splicing exist, such as alternative 5′ or 3′splice-site usage, differential inclusion or skipping of particular exons, mutually exclusion of exons, and more.[3] Importantly, alternative splicing is often tightly regulated in a cell type- or developmental stage-specific mode.[3] The essential nature of this process is underscored by the fact that misregulation (missplicing events) is often related to human disease.[4–6] The caldesmon gene (*CALD1*) is a single gene with transcriptional variance characterized by the recombination of different alternative splicing modes regulated by specific promoter activities.[7] The human *CALD1* shares common structural and expressional properties through mammals.[8,9] The gene is located on chromosome 7q33–34, consists of at least 15 exons and gives rise to two major classes of protein isoforms, ie, high molecular weight caldesmon (120 to 150 kd, *h*-CaD) and low molecular weight caldesmon (70 to 80 kd, *l*-CaD).[7,10] The conserved regions of all isoforms encoded by exon 2, 3a, and 5 to 15 contain caldesmons' capacity to bind to actin, tropomyosin, Ca (2+)-calmodulin, myosin, and phospholipids.[11] The exons 1, 3b, and 4 are alternatively spliced. Exon 3b encodes the central α helix which is absent from *l*-CaD. *h*-CaD isoforms are restricted to fully differentiated smooth muscle cells (SMCs) and regulate the smooth muscle tone. *l*-CaD consists of at least four splicing variants (WI-38 *l*-CaDs I and II, Hela *l*-CaDs I and II) which are expressed via differential inclusion of the variable alternative spliced exons 1, 1′ and 4 of the gene.[7] The exons 1 and 1′ encode the short amino terminus specific for Hela *l*-CaDs and WI-38 *l*-CaDs or *h*-CaD, respectively.[7] The *l*-CaD isoforms are ubiquitously distributed in various cells and dedifferentiated SMCs. They play roles in the regulation of cell contractility, adhesion-dependent

Accepted for publication February 23, 2004.

Address reprint requests to Johan M. Kros, M.D., Ph.D., Department of Pathology, Erasmus Medical Center, Office JNI Room 230-c, Dr. Molewaterplein 40, P.O. Box 2040, 3000 CA, Rotterdam, the Netherlands. E-mail: j.m.kros@erasmusmc.nl.

signaling, and cytoskeletal organization, influencing granule movement, hormone secretion, and reorganization of microfilaments during mitosis via mitosis-specific phosphorylation by cdc2 protein kinase.[10–12] The distinct functions of different cell types must involve different isoforms of caldesmon. However, the expression of the various *CALD1* splicing variants and protein isoforms has only been investigated in a limited selection of normal human tissues.[8] In human aorta, all splicing variants of the gene have been investigated. The expression was restricted to *h*-CaD (exon 1, 3b, and 4) and WI-38 *l*-CaD II (exon 1′).[8]

In glioma, microvascular proliferation or hyperplasia is a notorious event. Microvascular architecture and density in low-grade gliomas are similar to that in normal brain tissue. In anaplastic gliomas and glioblastomas however, microvascular hyperplasia such as glomeruloid and branching or sprouting proliferation, is a common event. Leakage of these vessels leads to perivascular edema and shows in neuroradiologic presentations of high-grade gliomas. The proliferated or hyperplastic vessels are dysfunctional in that there is a disruption of the blood-brain barrier.

In a previous study we found the low molecular isoform of caldesmon (*l-CaD*) in the cerebrospinal fluid (CSF) of glioma patients.[13] It was noticed by immunohistochemistry on tissue sections of the very gliomas that the expression of caldesmon was restricted to the blood vessels while no immunopositivity was obtained in glial cells. In the present study, we further investigated the *CALD1* splicing variants, focusing on *l-CaD* in tissue samples of 68 patients with gliomas. In order to localize the caldesmon protein in the tumors, immunohistochemistry was performed on tissue sections of the gliomas of the same patients from whom the CSF samples were used. The expression of caldesmon appeared to be restricted to the blood vessels and was not seen in glial cells. In addition, any possible or minor cellular components present in the normal controls and glioma samples were pre-screened by LCM/RT-PCR and immunohistochemistry. Missplicings in glioma microvessels are revealed by RT-PCR. The transcriptional changes consequently result in an up-regulated protein expression level. Alterations of splicing patterns could result from splice-site mutations via activation of cryptic splice-site usage.[16,17] The phenotypic effects of such mutations on mRNA splicing often cause codon frame-shifts or single base substitution consequently resulting in premature termination codons.[18,19] Such splice-site mutations account for at least 15% of point mutations causing disease in humans.[16,20] To rule out the presence of splice-site mutations resulting in the missplicing events of the *CALD1* gene in our tumor cases, the samples were scanned by coupled *in vitro* transcription/translation assay (IVTT, also known as the protein truncation test (PTT)). The principle of IVTT is based on targeting mutations that generate truncated proteins induced by premature translation termination.[21] IVTT enables to pinpoint the site of a mutation, offers good sensitivity, and a low false-positive rate.[22] Further tight junction proteins (occludin and ZO-1) were co-investigated in this study. Interestingly, the up-regulated expression of *l-CaD* resulting from *CALD1* missplicing was coincident with the down-regulation of occludin and ZO-1, causing tight junction (TJ) breakdown of the endothelial cells in glioma microvasculature.

Materials and Methods

Samples and Histology

The study was conducted on 68 snap-frozen specimens of glioma stored in the archives of the Department of Pathology, Erasmus Medical Center, Rotterdam, the Netherlands. Histopathological typing and grading of the tumors was performed on the corresponding paraffin sections based on the latest World Health Organization classification of tumors of the central nervous system.[23] Frozen section screening was to get rid of those samples with massive necrosis, hemorrhage, and contaminating normal tissues. Finally, the tumors analyzed included 26 glioblastomas, 23 oligodendrogliomas (among which 18 anaplastic oligodendrogliomas), and 19 pilocytic astrocytomas. Six samples of white matter obtained from patients without neurological or systemic disease served as controls.

Light Microscopy/Immunohistochemistry

To determine the site and distribution of the *l-CaD* protein expression in the tumors and control samples, tissue sections were immunohistochemically stained with a monoclonal anti-*l-CaD* antibody at a 1:40 dilution (BD Biosciences). The immunohistochemical procedure was described previously.[13]

Pre-Screening CALD1 Expression in All of the Cellular Components Possibly Present in the Tissue Samples Used by Laser-Capture Micodissection (LCM)/RT-PCR and Immunohistochemistry

The main purpose for the pre-screening experiments was to determine whether unfractional samples can be used for analysis. The white matter controls predominantly consist of glial cells and blood vessels with minor blood cell components. In glioma, the major cellular components are neoplastic glial cells (glioma cells) and hyperplastic or proliferated microvessels with possible or minor contaminating cells such as inflammatory cells, fibroblasts, and leptomeningeal cells. Normal glial cells and normal vessels were captured from the control samples (4 cases), while glioma cells and glioma vessels were captured from glioma cases (10 cases), respectively. Fibroblasts and leptomeningeal cells were captured from normal dura and arachnoid (two each from autopsy cases), respectively. Since all kinds of inflammatory cells are derived from transmigration of leukocytes from blood vessels into the brain tissue, 20 normal blood samples were used for screening of possible *CALD1* expression in

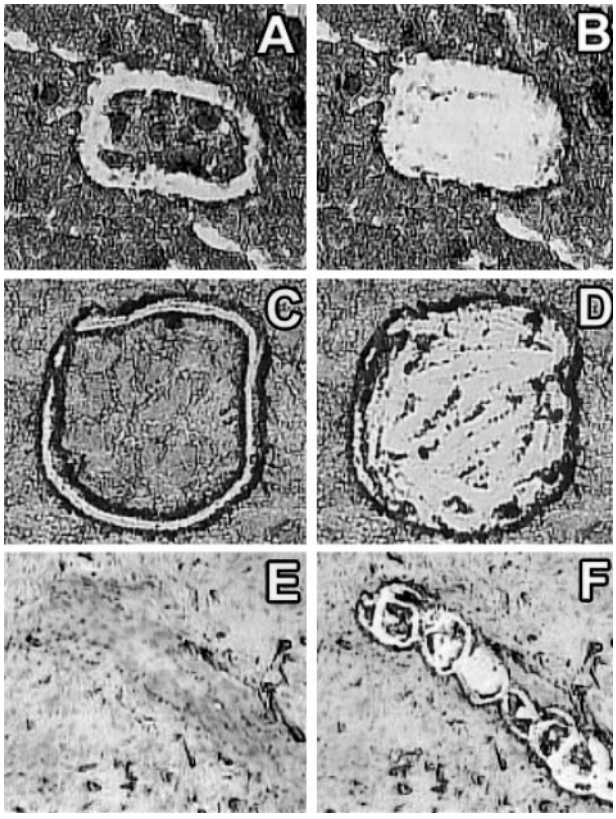

Figure 1. Laser-capture microdissection of glial cells and vessels. **A:** The target normal glial cell population was dissected with ultraviolet laser. **B:** The dissected cells were photo-ablated within the laser focus and then directly collected into a microcentrifuge tube cap filled with Trizol for RNA isolation by laser pressure catapulting. **C:** The target tumor cell population (glioblastoma) was dissected with ultraviolet laser. **D:** The dissected cells were photo-ablated and collected as mentioned under **B**. **E:** The targeted hyperplastic vessel in pilocytic astrocytoma was positioned. **F:** The dissected vessel was photo-ablated and collected as mentioned in (**B**).

leukocytes. LCM was performed by using a Robot Microbeam laser microscope as the manufacturer instructed (P.A.L.M, Microlaser Technologies, Bernried, Germany). Frozen sections for LCM were prepared by using Rnase-free conditions. The used frozen tissue blocks were sectioned at 5 μm in cryostat, mounted on non-coated clean glass sliders, and stored at −80°C until use. The staining procedures of the sections were mainly based on the published protocol at http://pathbox.wustl.edu/~tisscore/protocols.htm.[24] A slight modification of the protocol was made by skipping "automation buffer" and using the stainer (HisGene, Arcturus) instead of Mayer's hemotoxylin and eosin. For Robot Microbeam laser microdissection, the tissue area of interest was selected and positioned (Figure 1, A, C, and E), and cut out using a focused, pulsed laser beam. The dissected areas were collected in the cap of a microcentrifuge tube containing 18 μl Trizol (Invitrogen) via laser pressure catapulting. The object of interest was catapulted off the slide using a high-energy, defocused, short-duration laser pulse (Figure 1, B, D, and F). The cap with the procured tissues was immediately placed on a microcentrifuge tube containing 200 μl Trizol (Invitrogen) and lysed by mixing for further RNA isolation.

CALD1 Transcript Analysis

Total cellular RNA was extracted from the selected specimens using Trizol per the manufacturer's protocol (Invitrogen). First-strand complementary DNA (cDNA) was generated with an oligo $(dT)_{23}$ primer and DuraScript reverse transcriptase (Sigma). The resulting cDNA was amplified by PCR using *CALD1* specific primer sets spanning the splice sites of this gene toward all of the four splicing variants of *l-CaD* as described elsewhere.[7] A primer set for the *CALD1*, designed to amplify all of the splicing variants,[25] was used for initial examining the microdissected samples (the product size for *l-CaD* isoforms is 744 bp). Glyceraldehyde 3-phosphate dehydrogenase (*GAPD*) fragment[26] was prepared by PCR as an internal control. All of the primers used in this study were commercially synthesized (Invitrogen). The amount of each RNA sample used was selected on the basis of identical amounts of *GAPD* cDNA amplified from each sample. At a 2-minute initial denaturation at 94°C, amplification conditions were as follows: 94°C for 15 seconds, 66°C (60°C for GAPD) for 30 seconds and 68°C for 1 minute for 36 cycles (40 cycles for the microdissected samples), and final extension at 68°C for 5 minutes. *GAPD* transcripts were amplified by 30 cycles (36 cycles for the microdissected samples). Negative controls, consisting of one sample without reverse transcriptase and one without template, were included in each experiment. The PCR products were resolved by electrophoresis on a 1% agarose gel containing ethidium bromide, and viewed under ultraviolet illumination. At least three experiments were performed for reproducibility.

Immunoblotting

Total cellular protein was co-isolated and lysed during RNA isolation by Trizol according to the manufacturer's protocol (Invitrogen). Protein concentrations in the extracts were determined by the BCA protein assay (Pierce Chemical Co). Protein samples (15 μg/lane) were separated on a 12% SDS-polyacrylamide gel and transferred to nitrocellulose. Electroblotting was performed on a nitrocellulose membrane in 25 mmol/L Tris and 192 mmol/L glycine containing 20% methanol. The membrane was then pre-treated with 5% skim milk in Tris-buffered saline with Tween (TBST) overnight at 4°C. The membrane was incubated with monoclonal anti-*l-CaD* antibody (BD Biosciences, dilution 1:1000) in TBST or anti-α,β-tubulin cocktail (Lab Vision, dilution 1:1000) in TBST for 1 hour at room temperature. The membrane was further incubated with horseradish peroxidase (HRP)-conjugated goat anti-mouse IgG antibody (Zymed Laboratory Inc., dilution 1:10,000) for 1 hour at room temperature. The peroxidase was finally activated with enhanced chemiluminescence (ECL kit, Amersham) and the immunoreactivity was visualized with Kodak X-Omat AR X-ray film. For quantitative analysis of *l-CaD*, the bands on films were scanned by using a UMAX PowerLook II scanner (Genomic Solutions, Huntingdon, UK) at 750 dpi. Densitometric analysis was performed with the ONE-Dscan software (Scanalytics,

Billerica). Each experiment was repeated at least twice. The average change in band intensities was normalized against tubulin.

IVTT

The specimens used by a coupled *in vitro* transcription/translation assay (IVTT) were pre-treated by puromycin (200 μg/ml) (Sigma) for 6 hours at room temperature before RNA isolation. Puromycin is a translation inhibitor known to suppress nonsense-mediated mRNA decay (NMD), thus allowing mutation screening at the RNA level.[27] The PCR products suitable for IVTT analysis were generated with sense primers containing a T7 RNA polymerase promoter, a start condon, and the Kozak translation initiation sequence.[28] The transcripts were amplified by 40 cycles. Since the normal transcripts containing exons 1, 1 + 4, and 1′ + 4 were not detected in the control white matter, the corresponding transcripts used in IVTT were retrieved from normal stomach, prostate, and thyroid, respectively. The PCR product (2.5 μl) amplified from each transcript was incubated in the TNT/T7 non-radioactive coupled transcription and translation system (TNT Quick for PCR DNA, Promega) for 90 minutes at 30°C in a total volume of 50 μl in the presence of biotinylated lysine residues. The biotinylated lysine residues are incorporated into nascent protein during translation, eliminating the need for labeling with [^{35}S] methionine or other radioactive amino acids, and allowing non-radioactive detection of protein synthesized *in vitro* by binding either streptavidin-alkaline phosphatase (streptavidin-AP) or streptavidin-horseradish peroxidase (streptavidin-HRP). In our experiments, the *in vitro* synthesized proteins were size-fractionated on 12% SDS-polyacrylamide mini-gels. The fractionated proteins were electroblotted onto nitrocellulose at a constant voltage of 100V for 60 minutes. Streptavidin-HRP binding (dilution 1:20,000) was used for visualization with enhanced chemiluminescence (ECL kit, Amersham) as the protocol (Promega).

Expression of Occludin and ZO-1 in Glioma Microvasculature Detected by Immunofluorescence and Immunohistochemistry

Cryostat sections (5 μm) were cut onto non-coated microscope slides (Menzel-Glaser). Slides were fixed in 100% ice-acetone at room temperature for 10 minutes and air-dried. After washes with phosphate-buffered saline (PBS), indirect immunofluorescence was carried out by using the anti-occludin polyclonal antibody (Zymed Laboratories Inc., dilution 1:100) and anti-ZO-1 polyclonal antibody (Zymed Laboratories Inc., dilution 1:100) with incubation for 1 hour at room temperature. The FITC-conjugated swine anti-rabbit IgG (Dako, dilution 1:100) was used for 1 hour at room temperature for visualization. Slides were washed with PBS, mounted in imselmount (Klinipath), and covered with Pertex and covering glass. A CCD video camera (Leica) mounted on a Leica (DM-RXA) fluorescence microscope was used to capture digital images on a Leica computer (Q550 CW) running the software (Leica CW 4000 FISH Version V 1.0).

For immunohistochemistry, 5-μm paraffin sections were cut onto aminopropyltriethoxysilane (APES)-coated glass slides (Knittel Glaser). Dewaxed sections were pre-treated in 0.1% pronase (Sigma) for 10 minutes at 37°C. After the pre-treatment, the slides were washed with PBS and incubated with anti-occludin polyclonal antibody (Zymed Laboratories Inc., dilution 1:100) for 2 hours at room temperature. The biotinylated goat anti-rabbit (Dako, dilution 1:200) was used for 1 hour at room temperature for visualization. Again the slides were washed in PBS and incubated with StreptABC complex/AP (Dako, dilution 1:100) for 1 hour at room temperature. After the slides were washed with PBS, enzyme detection was performed by using a solution of Tris-HCl (pH 8.0) containing 1% new fuchsin, 1% natriumnitriet, 0.03% napthol AS-MX phosphate (Sigma), and 0.025% levamisol (Acros) for 1 hour at room temperature. The slides were washed again with PBS, mounted in imselmount (Klininpath), and covered with Pertex and covering glass for examination under a light microscope.

Results

Confirmation of Absent Expression of CALD1 Transcript and Protein in Glial Cells

Immunohistochemistry showed that the expression of the caldesmon protein was restricted to the blood vessels. The immunoreactivity for the caldesmon protein was stronger in the hyperplastic microvessels of the gliomas as compared to normal brain microvasculature (Figure 2, A to E). The enhanced immunoreactivity was confirmed by immunoblotting analysis showing a higher expression of total *l-CaD* in the tumor samples (see below). At the light microscopical level no immunopositivity was observed in neoplastic and normal glial cells in the specimens. Neither the neoplastic, nor the normal, glial cells captured by LCM showed expression of *CALD1* transcripts, in contrast to the positive controls (tumor vessels) (Figures 1 and 3).

Expression Profiles of CALD1 in Microdissected Normal Brain Vessels and Other Possible or Minor Cellular Components in Normal Controls and Gliomas

The microdissected microvessels from the normal controls showed expression of exon 1′(WI-38 II) (Figure 4). Fibroblasts express *CALD1* with restriction to exon 1′ and with immunopositivity of caldesmon (Figure 5). Further, no *CALD1* expression was found in leptomeningeal cells by LCM/RT-PCR and immunohistochemistry (Figure 6). No *CALD1* expression in leukocytes or inflammatory cells was detected (Figure 7).

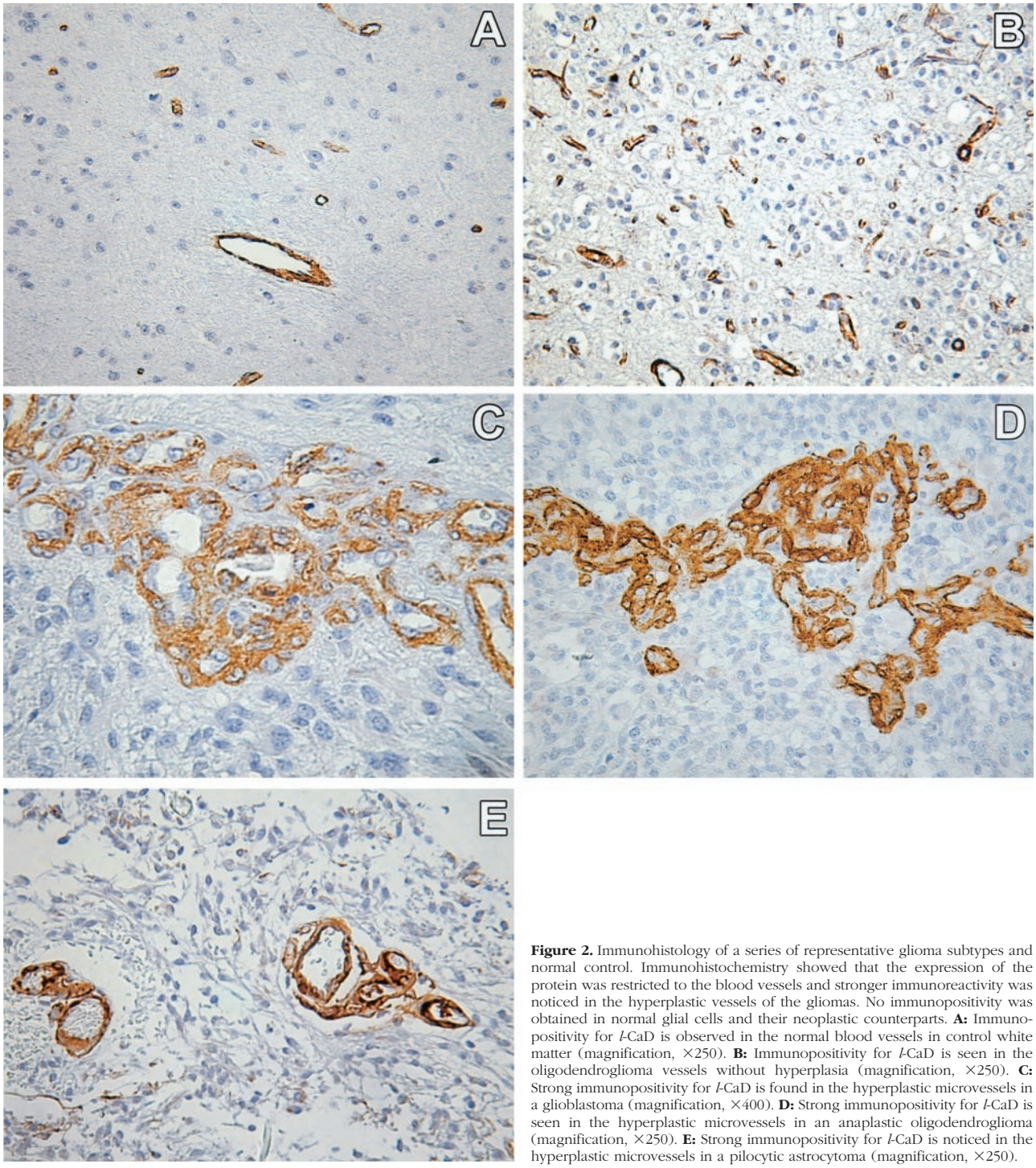

Figure 2. Immunohistology of a series of representative glioma subtypes and normal control. Immunohistochemistry showed that the expression of the protein was restricted to the blood vessels and stronger immunoreactivity was noticed in the hyperplastic vessels of the gliomas. No immunopositivity was obtained in normal glial cells and their neoplastic counterparts. **A:** Immunopositivity for *l*-CaD is observed in the normal blood vessels in control white matter (magnification, ×250). **B:** Immunopositivity for *l*-CaD is seen in the oligodendroglioma vessels without hyperplasia (magnification, ×250). **C:** Strong immunopositivity for *l*-CaD is found in the hyperplastic microvessels in a glioblastoma (magnification, ×400). **D:** Strong immunopositivity for *l*-CaD is seen in the hyperplastic microvessels in an anaplastic oligodendroglioma (magnification, ×250). **E:** Strong immunopositivity for *l*-CaD is noticed in the hyperplastic microvessels in a pilocytic astrocytoma (magnification, ×250).

Differential Expression of CALD1 Transcripts and Protein in Glioma Microvessels versus *Normal Brain Microvasculature*

The results of immunohistochemistry and the LCM data revealed that there was no expression of protein and transcript of the *CALD1* gene in normal and neoplastic glial cells. In addition, the pre-screening experiments show that no differential expression patterns of *CALD1* were detected in any of these cell types. Thus, it is feasible to use unfractional samples of control tissue (white matter) and glioma samples. Sixty-eight glioma samples were assessed by RT-PCR. The transcript containing exon 1′ (752 bp, WI-38 *l-CaD* II) was invariably detected in all tumors and control samples, while the transcripts containing the exons 1 (731 bp, Hela *l-CaD* II), 1 + 4 (670 bp, Hela *l-CaD* I), and 1′ + 4 (691 bp, WI-38 *l-CaD* I) were exclusively detected in the tumors (Figure 8

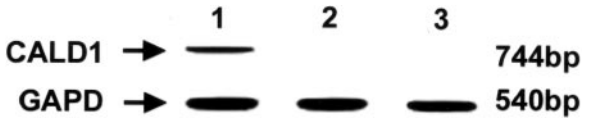

Figure 3. Analysis of *CALD1* transcript expression in purified glial cells by LCM. The used primer set was designed to amplify all of the splicing variants. **Lane 1** represents the positive control (tumor vessels; Figure 1, E and F) showing *CALD1* transcript expression (744 bp). **Lane 2** (normal glial cells) and **lane 3** (neoplastic glial cells) show no expression of *CALD1* transcripts. The housekeeping gene (*GAPD*) was identically amplified in all of the samples.

and Table 1). The transcript of the ubiquitously expressed housekeeping gene *GAPD* (540 bp) was uniformly amplified in all of the used samples. The splicing patterns show various frequencies and combinations of the expressed transcripts (Table 1). The expression pattern of *l-CaD* in normal brain vessels is similar to that of the human normal aorta cDNA.[8] The expression of the additional transcripts in the gliomas appears to be tightly linked with the presence of microvascular hyperplasia or proliferation in the sample examined. The samples with normal-looking microvessels retained normal expression patterns of *CALD1*. The findings in the microdissected vessels (4 of 6 controls and 10 of 68 gliomas) further confirmed the results from these unfractional samples. To determine whether the change in *l-CaD* transcription would be manifested as changes in the protein quantity, immunoblotting analysis was performed on total cell lysates of the glioma and control samples. Densitometric analysis revealed an average 3.6-fold enhancement of caldesmon protein levels in the tumor samples as compared to the normal controls (Figure 9), indicating that the transcriptional changes were translated into altered protein levels.

Splice-Site Mutation Scanning

Mutation screening was carried out on 20 glioma cases by applying the IVTT to exon 1, exon 1′, and exon 4, spanning all splice sites for each transcript. No mutations leading to premature protein terminations were observed in these target exons (Figure 10).

Tight Junction Breakdown in Glioma Microvasculature

The expression of TJ proteins (occludin and ZO-1) was detected by immunohistochemistry (IH) and immunoflu-

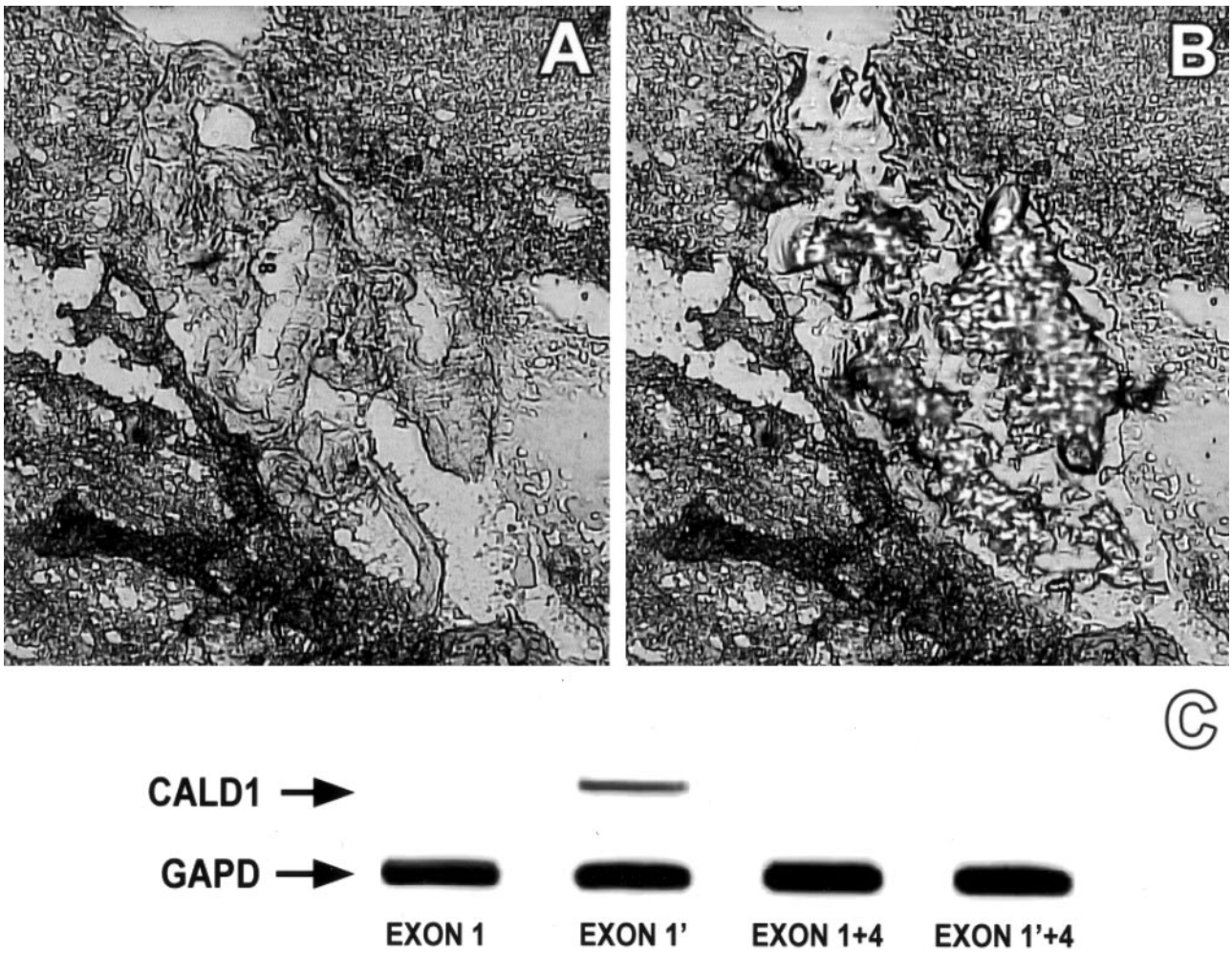

Figure 4. Laser-capture microdissection of normal brain vessels. **A:** Normal brain vessels before microdisection. **B**: The target vessels from A after microdissection. **C:** The RT-PCR results from the microdissected vessels. These normal vessels express exon 1′ only.

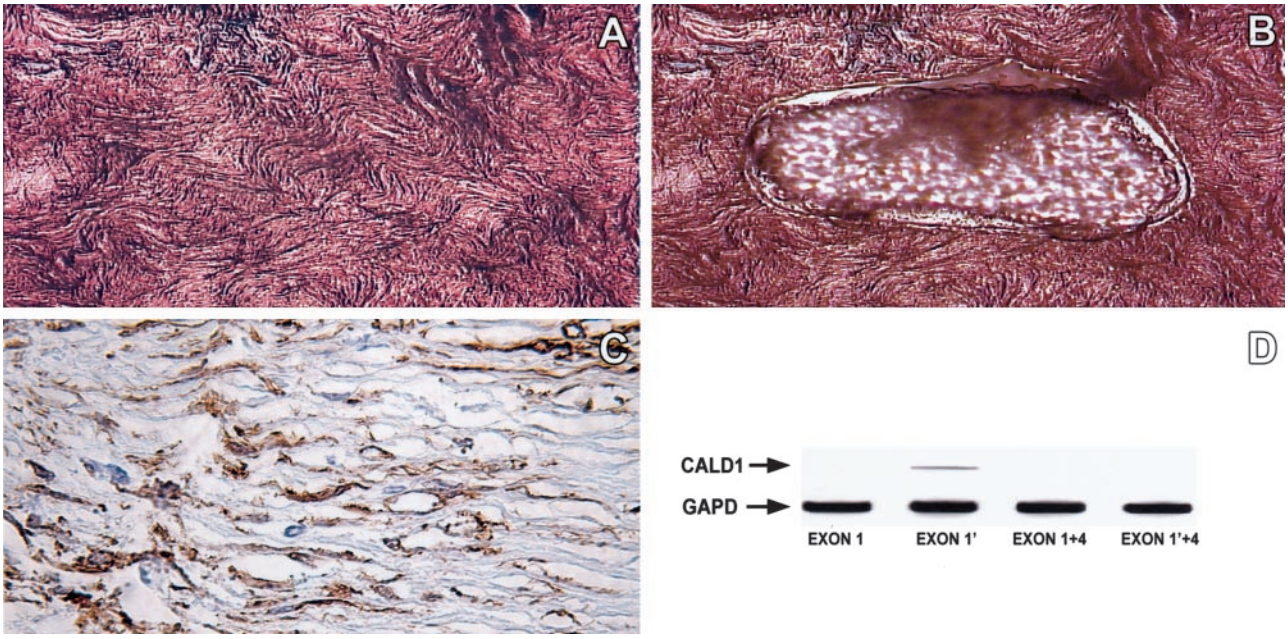

Figure 5. Laser-capture microdissection of fibroblasts from normal dura. **A:** Normal dura before microdissection. **B:** The microdissected target cell population from A. **C:** Positive immunoreactivity for caldesmon is shown in the fibroblasts. **D:** The RT-PCR results from the micodissected fibroblasts. The fibroblasts show *CALD1* expression with restriction to exon 1′.

orescence (IF). Occludin and ZO-1 in our study showed similar expression patterns (data from ZO-1 not shown). In longitudinally sectioned normal blood vessels, the staining patterns for occludin and ZO-1 were predominantly axial and linear, with occasional anastomoses/bifurcations (Figure 11, A1 and A2). In transversely sectioned vessels, however, the staining revealed short, radial or near-radial, continuous staining bands (Figure 11, B1 and B2). In the proliferated and/or hyperplastic glioma microvessels abnormalities in expression of occludin and ZO1 were observed. The abnormalities include reduced clarity of TJ bands (Figure 11, C1 and C2), interruption or discontinuity (Figure 11, D1 and D2), beading or spot-like pattern of the TJ staining (Figure 11E), or diffuse intracytoplasmic staining or absence or complete loss of immunostaining (Figure 11F).

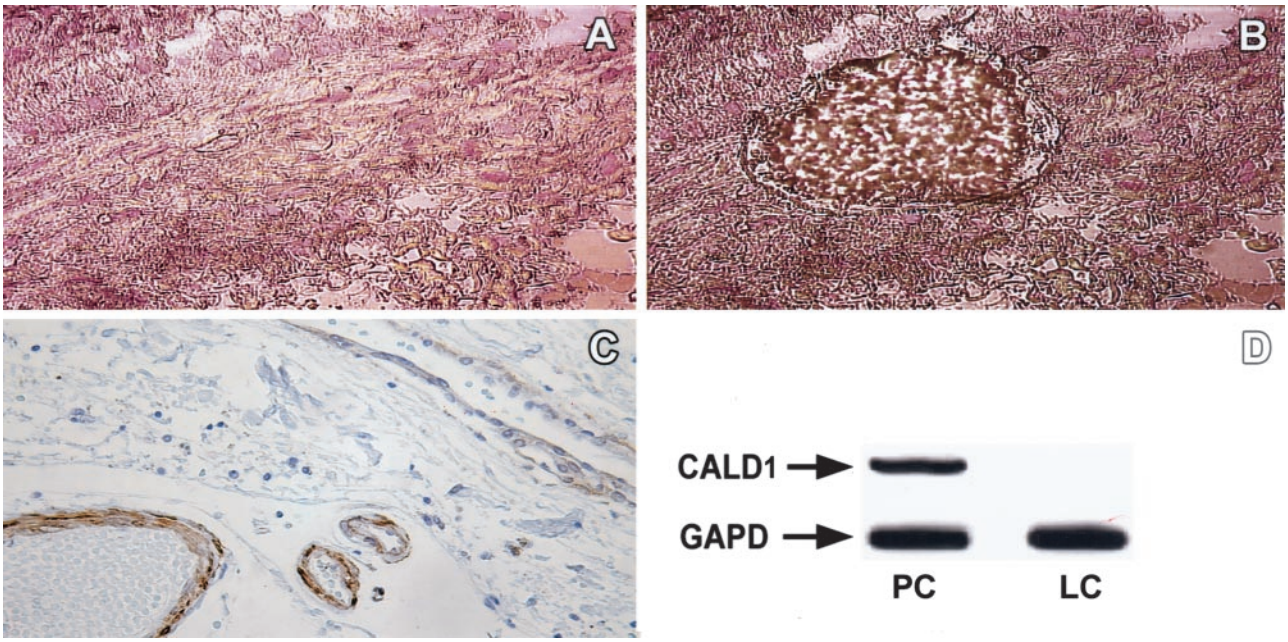

Figure 6. Laser-capture microdissection of normal leptomeningeal cells from the arachnoid. **A:** Normal arachnoid before microdissection. **B:** The microdissected target leptomeningeal cell population from **A**. **C:** No immunoreactivity for caldesmon is seen in the leptomeningeal cells. **D:** The RT-PCR results from the micodissected leptomeningeal cells. PC, positive control; LC, leptomingeal cells. The housekeeping gene (*GAPD*) was identically amplified in the PC and LC. No expression of *CALD1* transcript in leptomeningeal cells was found.

Figure 7. Examination of *CALD1* expression in leukocytes or inflammatory cells. A representative RT-PCR result of the blood samples is shown. PC, positive control; B1 to B6, blood samples examined. The housekeeping gene (*GAPD*) was identically amplified in all of the samples examined. No *CALD1* expression was found in the leukocytes or inflammatory cells.

Correlation of Up-Regulation of l-CaD Resulting from CALD1 Missplicing and TJ Breakdown in Glioma Microvasculature

The up-regulation of *l-CaD* resulting from *CALD1* missplicing in hyperplastic glioma microvasculature is coincident with down-regulation of occludin (Figure 12) and ZO-1. In our study, strong immunopositivity of *l-CaD* in hyperplastic glioma microvasculature was always concomitant with complete or near-complete loss of occludin and ZO-1 expression.

Discussion

Tumor vessels are morphologically and functionally different from normal vasculature.[29] The endothelial cells

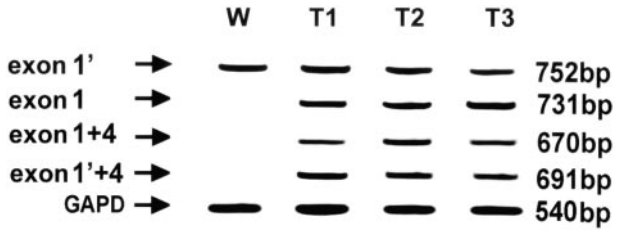

Figure 8. Analysis of *CALD1* splicing transcripts. Total RNA was isolated from the tumors and controls, and subjected to RT-PCR analysis. The expressed transcript variants and the corresponding sizes are indicated on the left and right, respectively. Each lane was labeled as W (white matter), T1 (glioblastoma), T2 (anaplastic oligodendroglioma), and T3 (pilocytic astrocytoma), respectively. The housekeeping gene (*GAPD*) was identically amplified in all samples. The transcript containing exon 1′ is invariably co-detected in the control and tumors, while the transcripts containing exon 1, 1 + 4, and 1′ + 4 are exclusively expressed in the tumor samples.

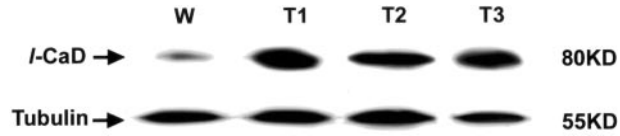

Figure 9. Immunoblotting analysis of *l-CaD*. The labels of the consecutive lanes correspond to those in Figure 8. Enhanced *l-CaD* protein expression is revealed in the tumors as compared to the control. Tubulin expression was used as a total protein loading control. The average change in band intensities was normalized against tubulin signal.

are mitotically active and there is enhanced permeability of the micovascular walls.[30] Nevertheless, there is substantial difference in neoplastic angiogenesis between tumor types, depending on the organ system involved and differential expression of cytokines by organ-specific stroma.[31,32] In the brain, the microvascular system is composed of endothelial cells surrounded by a layer of pericytes.[33] The lack of smooth muscle cells in brain tissue suggests that any contractile activity must be performed by either endothelial cells, pericytes, or both. The development of glioma microvasculature may serve as a typical model of neoplastic angiogenesis. In particular, glioblastoma are among the best-vascularized tumors in humans with highest endothelial cell proliferation indices.[23,32] Numerous factors such as angiopoietins and their Tie receptors,[34] PDGF-B,[35] monocyte chemotactic protein 1,[36] ephrins, and Eph-B receptors[37,38] are likely candidates for the activation of various modes of angiogenesis, and mediation of endothelial-endothelial and endothelial-pericyte interactions in the adaptation to physiological and pathological stimuli.[39] So far, the caldesmon protein has not yet been implicated in angiogenesis.

Caldesmon is an actomyosin-associated cytoskeletal protein residing in contractile microfilaments (MFs).[10] The actin cytoskeleton in eukaryotic cells operates as a tension-sensing molecular device and has an important regulatory role on cellular contractility and adhesion-dependent signaling via caldesmon modulation.[40] The contractile functions are carried out by modulating cellular tensional integrity (tensegrity) without disrupting the cel-

Table 1. Summary of Differential Expression Patterns of *CALD1* Transcripts in Gliomas *versus* the Controls

Case no.	Glioma subtypes	Expression patterns			
		Hela II (exon 1)	WI-38 II (exon 1′)	Hela I (exon 1 + 4)	WI-38 I (exon 1′ + 4)
Controls			+		
1–8	Glioblastoma	+	+	+	+
9–17	Glioblastoma	+	+		+
18–26	Glioblastoma		+		+
27–32	Anaplastic oligodendroglioma	+	+	+	+
33–34	Anaplastic oligodendroglioma	+	+	+	
35–38	Anaplastic oligodendroglioma	+	+		+
39–40	Oligodendroglioma	+	+		+
41	Oligodendroglioma	+	+		
42–47	Anaplastic oligodendroglioma		+		+
48–49	Oligodendroglioma		+		
50–56	Pilocytic astrocytoma	+	+	+	+
57–58	Pilocytic astrocytoma	+	+		+
59–61	Pilocytic astrocytoma	+	+		
62–63	Pilocytic astrocytoma		+		+
64–68	Pilocytic astrocytoma		+		

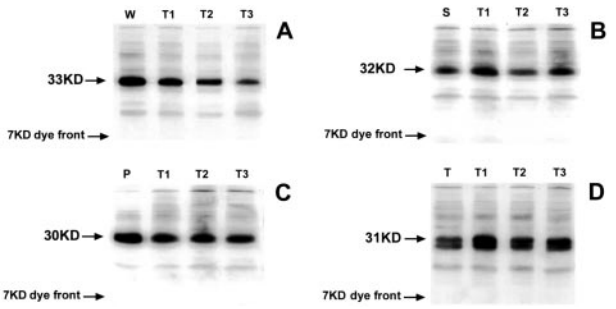

Figure 10. Scanning of splice-site mutations. The four panels show the IVTT analysis of the representative cases corresponding to Figures 8 and 9. The wild polypeptides synthesized *in vitro* contain exon 1′ from white matter indicated as "W" (**A**), exon 1 from stomach indicated as "S" (**B**), exon 1 + 4 from prostate indicated as "P" (**C**) and exon 1′ + 4 from thyroid indicated as "T" (**D**). The predicted MWs of these polypeptides are indicated in kd. No truncated polypeptides are observed in the glioma cases as compared to the controls. **D** displays a mass heterogeneity by two bands. This mass heterogeneity is possibly caused by the inclusion or exclusion of exon 4, or alternatively, by an internal ATG initiation site.

lular structural integrity.[41] However, alterations of *CALD1* expression and the molecular mechanisms leading to such alterations in the context of neoplastic angiogenesis remain unexplored. Based on our previous findings,[13] we hypothesized that the enhanced protein expression in glioma cases is regulated at the transcriptional level, not just simply reflecting post-translational modifications of the protein. Definitely, the analysis of transcriptional changes could potentially lead to the identification of novel transcription-dependent and -independent molecular contributors to the process of neoplastic neovascularization. To address this issue, we investigated the *CALD1* splicing transcripts and expression level of this protein. Our data indicate that the transcriptional changes of *CALD1* in splicing variants are translated into altered protein levels, and both the expression of the splicing variants and the protein are up-regulated during the process of neo-angiogenesis in gliomas. In non-muscle cells, simulation of *CALD1* overexpression by transfection of full-length *l*-CaD results in the inhibition of cell contractility and interferes with Rho A-mediated formation of stress fibers and focal adhesions.[40] The co-activated caldesmon isoforms induce an overexpression of the protein and could have a synergetic effect on the cellular contractility of the vascular components, enhancing the permeability of microvessels, and consequently facilitate the extravasation and migration of cancer cells. Moreover, both an increase in cellular calcium concentration and caldesmon phosphorylation cause dissociation of

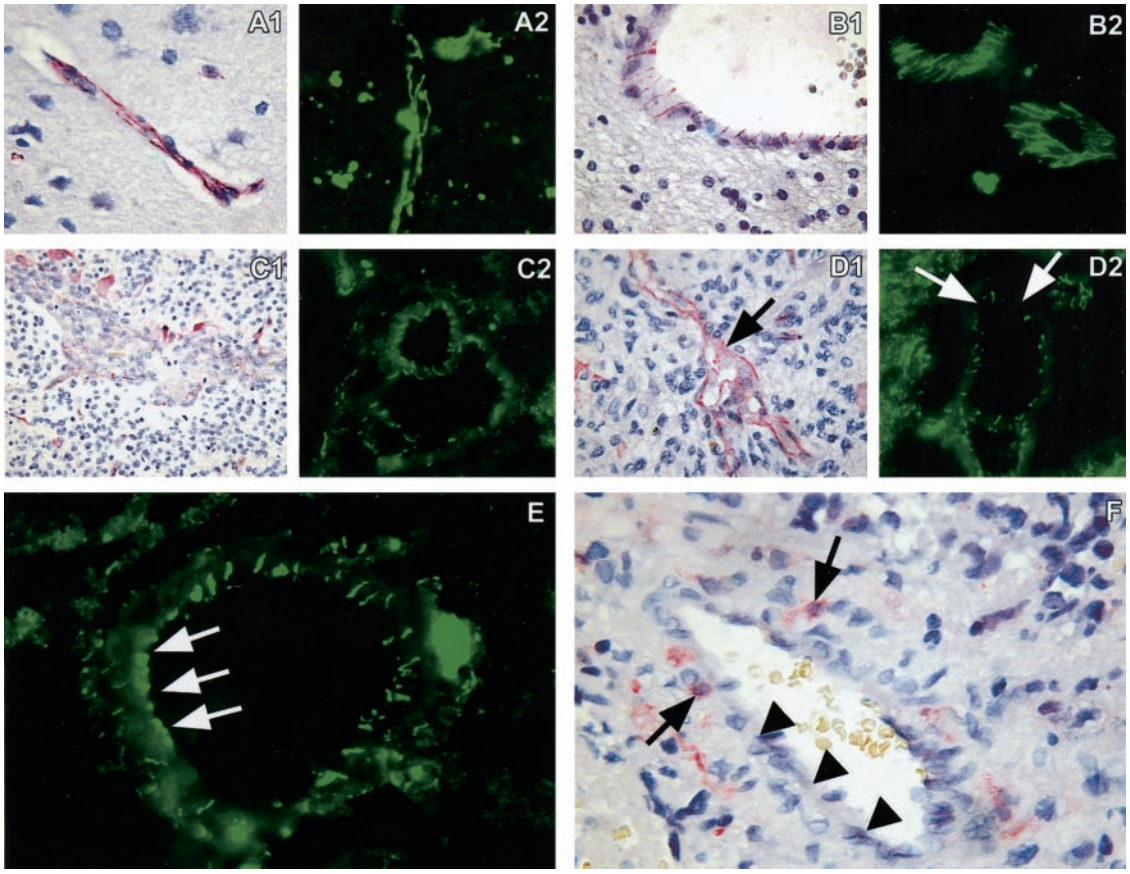

Figure 11. Immunofluorescence (IF) and immunohistochemical (IH) staining of occludin. **A1**, **B1**, **C1**, **D1**, and **E** show IH images, while **A2**, **B2**, **C2**, **D2**, and **F** exhibit IF images. **A1** and **A2:** Immunoreactive pattern for occludin in a longitudinal section of normal brain vessels (magnification, ×250). The vessels show an axial and linear staining pattern with occasional anastomoses or bifurcations. **B1** and **B2:** Immunoreactive pattern for occludin in a transverse section of normal brain vessels, characterized by short, radial or near-radial, continuous staining bands (magnification, ×250). **C1** and **C2:** Hyperplastic glioma vessels immunostained for occludin, showing reduced clarity of TJ patterns (magnification, C1 ×100; C2 ×250). **D1** and **D2:** Discontinous immunostaining for occludin in a glioma vessel (**arrows**) (magnification, ×250). **E:** Glioma vessel with spot-like or beading immunostaining pattern for occludin (**arrows**) (magnification, ×250). **F:** Redistribution of occludin immunoreactivity in the endothelial cytoplasm (**arrows**) and complete loss of occludin staining (**arrowheads**) (magnification, ×400).

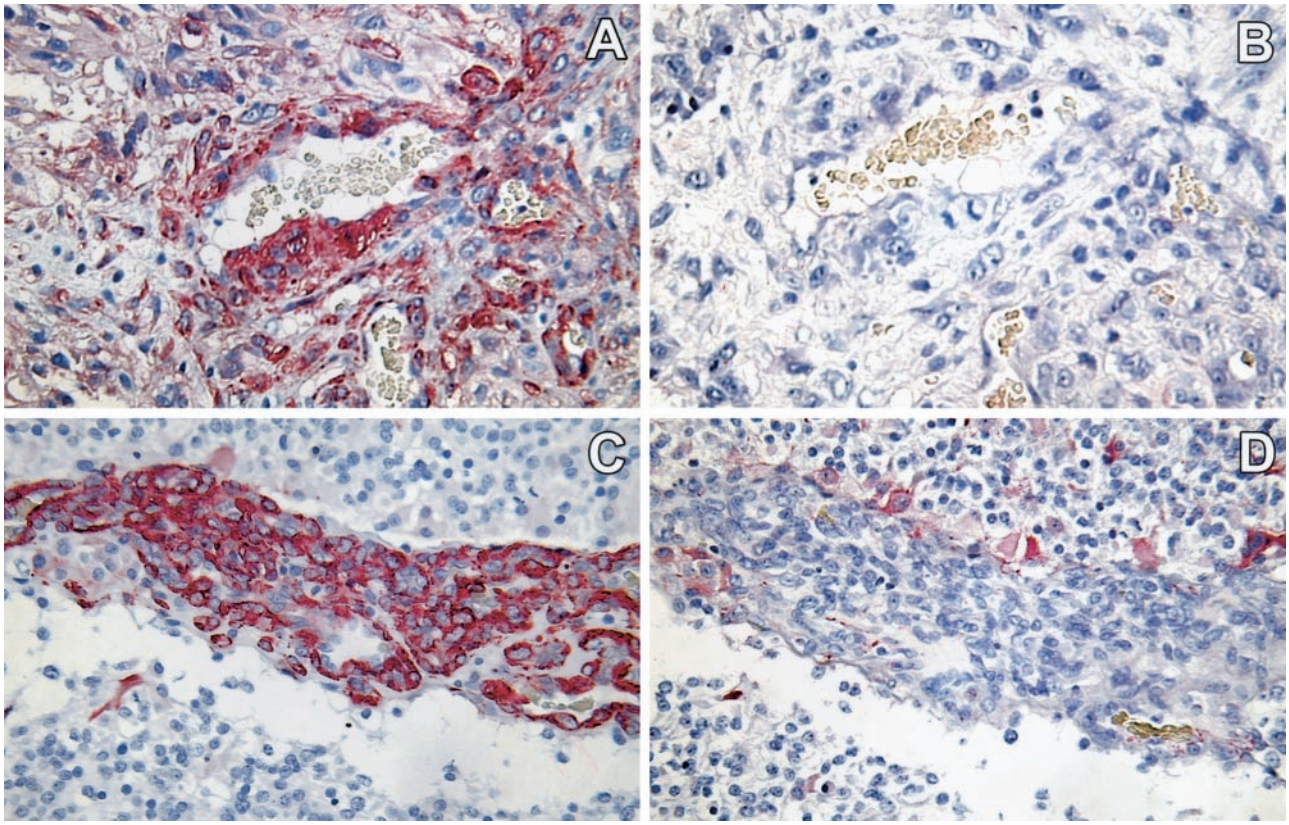

Figure 12. Up-regulation of *l-CaD* resulting from *CALD1* missplicing coincident with down-regulation of occludin. **A:** A glioblastoma with expression of four splice variants of *CALD1* (Case 6, Table 1). The strong immunoreactivity of *l-CaD* is observed (magnification, ×250). **B:** An adjacent section from **A** was immunostained for occludin. Complete loss of occludin immunoreactivity is observed (magnification, ×250). **C:** An anaplastic oligodendroglioma with expression of four splice variants of *CALD1* (Case 28, Table 1). Strong immunoreactivity of *l-CaD* is noticed in this section (magnification, ×250). **D:** An adjacent section immunostained for occludin. Near-complete loss of occludin expression is observed (magnification, ×250). In addition, the occludin redistribution in endothelial cytoplasm and ingestion by glial cells are shown.

caldesmon from actin and results in weakening most of caldesmon's properties.[10] Thus, it seems that caldesmon carries out a regulatory role in endothelial cell spread and elongation, two properties related to vascular development.[42–44] There is evidence from *in vitro* experiments that the expression of *CALD1* both at the transcriptional and translational level was markedly and reproducibly down-regulated during vascular tube formation.[45] Taken together, caldesmon appears to be a target in a variety of signaling pathways that modulate its function and thereby its effect on cell contractility and adhesion-dependent signaling.[40]

Alternative splicing of specific pre-mRNAs is controlled by *cis*-acting regulatory elements (exonic splicing enhancers) and *trans*-acting factors (SR proteins).[3] The alternative exons are commonly weakened as compared to constitutive exons by having suboptimal splice sites and length but are strengthened by the presence of exon enhancers that bind to putative splicing regulators[46] and/or activation of cryptic splice sites by mutation.[16] We did not trace any splice-site mutations in the examined cases. It appears that an alternative mechanism may alter the interaction between an exonic splice enhancer and mRNA splicing factors of the *CALD1* via a signaling pathway modifying the splicing apparatus.[2,47,48] The regulation of the transcriptional activation of *CALD1* splicing variants could have far-reaching epigenetic effects on the development of molecular targeted anti-angiogenic therapies.

The tight junction is the most apical located element of the junctional complex in epithelial and endothelial cells.[49] The TJ between endothelial cells of brain capillaries form the structural basis of the blood-brain barrier (BBB), which controls the exchange of molecules between blood and CNS. The endothelial cells of the normal blood-brain barrier possess tight junctions that maintain a severely restricted permeability. In the hyperplastic glioma microvasculature morphological alterations such as fenestrations, the increase of caveolae, pericyte detachment, and thickening and alteration of the extracellular matrix (ECM) exist.[50–52] These changes result in a dramatic increase of the permeability of these vessels. Occudin and ZO-1 are well-studied TJ proteins. In particular, occludin was the first identified transmembrane protein that is exclusively localized at TJ.[53] Therefore, occludin is considered a sensitive and reliable marker of TJs.[54] The inverse relationship between the regulation of *l-CaD* and occludin or ZO-1 found in our study has not yet been reported so far. Our data clearly reveal the up-regulation of *l-CaD* resulting from *CALD1* missplicing in hyperplastic glioma microvessels with a concomitant loss of TJ integrity of the endothelial cells. Although the mo-

lecular basis for this correlation remains unclear, our data are indicative of a specific contribution of *CALD1* expression patterns to glioma angiogenesis and generate hypotheses regarding the mechanisms contributing to the dysfunctionality of glioma neovascularization.

Acknowledgments

We thank Mr. F. van de Panne for his assistance with the photography.

References

1. Modrek B, Lee C: A genomic view of alternative splicing. Nat Genet 2002, 30:13–19
2. Grabowski PJ, Black DL: Alternative RNA splicing in the nervous system. Prog Neurobiol 2001, 65:289–308
3. Smith CW, Valcarcel J: Alternative pre-mRNA splicing: the logic of combinatorial control. Trends Biochem Sci 2000, 25:381–388
4. Philips AV, Cooper TA: RNA processing and human disease. Cell Mol Life Sci 2000, 57:235–249
5. Stoss O, Stoilov O, Daoud R, Hartmann AM, Olbrich M, Stamm S: Misregulation of pre-mRNA splicing that causes human diseases. Gene Ther Mol Biol 2000:9–28
6. Stoilov P, Meshorer E, Gencheva M, Glick D, Soreq H, Stamm S: Defects in pre-mRNA processing as causes of and predisposition to diseases. DNA Cell Biol 2002, 21:803–818
7. Hayashi K, Yano H, Hashida T, Takeuchi R, Takeda O, Asada K, Takahashi E, Kato I, Sobue K: Genomic structure of the human caldesmon gene. Proc Natl Acad Sci USA 1992, 89:12122–12126
8. Payne AM, Yue P, Pritchard K, Marston SB: Caldesmon mRNA splicing and isoform expression in mammalian smooth-muscle and nonmuscle tissues. Biochem J 1995, 305:445–450
9. Haruna M, Hayashi K, Yano H, Takeuchi O, Sobue K: Common structural and expressional properties of vertebrate caldesmon genes. Biochem Biophys Res Commun 1993, 197:145–153
10. Huber PA: Caldesmon. Int J Biochem Cell Biol 1997, 29:1047–1051
11. Bryan J: Caldesmon: fragments, sequence, and domain mapping. Ann NY Acad Sci 1990, 599:100–110
12. Yamakita Y, Yamashiro S, Matsumura F: Characterization of mitotically phosphorylated caldesmon. J Biol Chem 1992, 267:12022–12029
13. Zheng PP, Luider TM, Rob P, Avezaat CJJ, van den Bent MJ, Sillevis Smitt PAE, Kros JM: Identification of tumor-related proteins by proteomic analysis of cerebrospinal fluid from patients with primary brain tumors. J Neuropathol Exp Neurol 2003, 62:855–862
14. Garcia-Sanz JA, Mikulits W, Livingstone A, Lefkovits I, Mullner EW: Translational control: a general mechanism for gene regulation during T cell activation. EMBO J 1998, 12:299–306
15. Steger K: Haploid spermatids exhibit translationally repressed mRNAs. Anat Embryol (Berl) 2001, 203:323–334
16. Krawczak M, Reiss J, Cooper DN: The mutational spectrum of single base-pair substitutions in mRNA splice junctions of human genes: causes and consequences. Hum Genet 1992, 90:41–54
17. Stamm S: Signals and their transduction pathways regulating alternative splicing: a new dimension of the human genome. Hum Mol Genet 2002, 11:2409–2416
18. Cooper TA, Mattox W: The regulation of splice-site selection, and its role in human disease. Am J Hum Genet 1997, 61:259–266
19. van der Luijt RB, Khan PM, Vasen HF, Tops CM, van Leeuwen-Cornelisse IS, Wijnen JT, van der Klift HM, Plug RJ, Griffioen G, Fodde R: Molecular analysis of the APC gene in 105 Dutch kindreds with familial adenomatous polyposis: 67 germline mutations identified by DGGE, PTT, and southern analysis. Hum Mutat 1997, 9:7–16
20. Nakai K, Sakamoto H: Construction of a novel database containing aberrant splicing mutations of mammalian genes. Gene 1994, 141: 171–177
21. Bateman JF, Freddi S, Lamande SR, Byers P, Nasioulas S, Douglas J, Otway R, Kohonen-Corish M, Edkins E, Forrest S: Reliable and sensitive detection of premature termination mutations using a protein truncation test designed to overcome problems of nonsense-mediated mRNA instability. Hum Mutat 1999, 13:311–317
22. Den Dunnen JT, Van Ommen GJ: The protein truncation test: a review. Hum Mutat 1999, 14:95–102
23. Kleihues P, Louis DN, Scheithauer BW, Rorke LB, Reifenberger G, Burger PC, Cavenee WK: The WHO classification of tumors of the nervous system. J Neuropathol Exp Neurol 2002, 61:215–225; 226–219
24. Luzzi V, Holtschlag V, Watson MA: Expression profiling of ductal carcinoma in situ by laser-capture microdissection and high-density oligonucleotide arrays. Am J Pathol 2001, 158:2005–2010
25. Yamamura H, Yoshikawa H, Tatsuta M, Akedo H, Takahashi K: Expression of the smooth muscle calponin gene in human osteosarcoma and its possible association with prognosis. Int J Cancer 1998, 79:245–250
26. Shibuta K, Begum NA, Mori M, Shimoda K, Akiyoshi T, Barnard GF: Reduced expression of the CXC chemokine hIRH/SDF-1α mRNA in hepatoma and digestive tract cancer. Int J Cancer 1997, 73:656–662
27. Andreutti-Zaugg C, Scott RJ, Iggo R: Inhibition of nonsense-mediated messenger RNA decay in clinical samples facilitates detection of human MSH2 mutations with an in vivo fusion protein assay and conventional techniques. Cancer Res 1997, 57:3288–3293
28. Hogervorst FB, Cornelis RS, Bout M, van Vliet M, Oosterwijk JC, Olmer R, Bakker B, Klijn JG, Vasen HF, Meijers-Heijboer H, Menko FH, Cornelisce CJ, de Dunnen JT, Devilee P, Van Ommen G-JB: Rapid detection of BRCA1 mutations by the protein truncation test. Nat Genet 1995, 10:208–212
29. Krylova NV: Characteristics of microcirculation in experimental tumours. Bibl Anat 1969, 10:301–303
30. Carmeliet P, Jain RK: Angiogenesis in cancer and other diseases. Nature 2000, 407:249–257
31. Brat DJ, Van Meir EG: Glomeruloid microvascular proliferation orchestrated by VPF/VEGF: a new world of angiogenesis research. Am J Pathol 2001, 158:789–796
32. Eberhard A, Kahlert S, Goede V, Hemmerlein B, Plate KH, Augustin HG: Heterogeneity of angiogenesis and blood vessel maturation in human tumors: implications for antiangiogenic tumor therapies. Cancer Res 2000, 60:1388–1393
33. Ehler E, Karlhuber G, Bauer HC, Draeger A: Heterogeneity of smooth muscle-associated proteins in mammalian brain microvasculature. Cell Tissue Res 1995, 279:393–403
34. Folkman J, D'Amore PA: Blood vessel formation: what is its molecular basis? Cell 1996, 87:1153–1155
35. Hellstrom M, Kal n M, Lindahl P, Abramsson A, Betsholtz C: Role of PDGF-B and PDGFR-β in recruitment of vascular smooth muscle cells and pericytes during embryonic blood vessel formation in the mouse. Development 1999, 126:3047–3055
36. Shyy YJ, Hsieh HJ, Usami S, Chien S: Fluid shear stress induces a biphasic response of human monocyte chemotactic protein 1 gene expression in vascular endothelium. Proc Natl Acad Sci USA 1994, 91:4678–4682
37. Gale NW, Baluk P, Pan L, Kwan M, Holash J, DeChiara TM, McDonald DM, Yancopoulos GD: Ephrin-B2 selectively marks arterial vessels and neovascularization sites in the adult, with expression in both endothelial and smooth-muscle cells. Dev Biol 2001, 230:151–160
38. Shin D, Garcia-Cardena G, Hayashi S, Gerety S, Asahara T, Stavrakis G, Isner J, Folkman J, Gimbrone Jr MA, Anderson DJ: Expression of ephrinB2 identifies a stable genetic difference between arterial and venous vascular smooth muscle as well as endothelial cells, and marks subsets of microvessels at sites of adult neovascularization. Dev Biol 2001, 230:139–150
39. Burri PH, Djonov V: Intussusceptive angiogenesis: the alternative to capillary sprouting. Mol Aspects Med 2002, 23:1–27
40. Helfman DM, Levy ET, Berthier C, Shtutman M, Riveline D, Grosheva I, Lachish-Zalait A, Elbaum M, Bershadsky AD: Caldesmon inhibits nonmuscle cell contractility and interferes with the formation of focal adhesions. Mol Biol Cell 1999, 10:3097–3112
41. Ingber DE: Tensegrity I: Cell structure and hierarchical systems biology. J Cell Sci 2003, 116:1157–1173
42. Alessandro R, Masiero L, Lapidos K, Spoonster J, Kohn EC: Endothelial cell spreading on type IV collagen and spreading-induced FAK phosphorylation is regulated by Ca2+ influx. Biochem Biophys Res Commun 1998, 248:635–640
43. Masiero L, Lapidos KA, Ambudkar I, Kohn EC: Regulation of the RhoA

pathway in human endothelial cell spreading on type IV collagen: role of calcium influx. J Cell Sci 1999, 112:3205–3213
44. King WG, Mattaliano MD, Chan TO, Tsichlis PN, Brugge JS: Phosphatidylinositol 3-kinase is required for integrin-stimulated AKT and Raf-1/mitogen-activated protein kinase pathway activation. Mol Cell Biol 1997, 17:4406–4418
45. Grove AD, Prabhu VV, Young BL, Lee FC, Kulpa V, Munson PJ, Kohn EC: Both protein activation and gene expression are involved in early vascular tube formation in vitro. Clin Cancer Res 2002, 8:3019–3026
46. Humphrey MB, Bryan J, Cooper TA, Berget SM: A 32-nucleotide exon-splicing enhancer regulates usage of competing 5′ splice sites in a differential internal exon. Mol Cell Biol 1995, 15:3979–3988
47. Hoffmeyer S, Nurnberg P, Ritter H, Fahsold R, Leistner W, Kaufmann D, Krone W: Nearby stop codons in exons of the neurofibromatosis type 1 gene are disparate splice effectors. Am J Hum Genet 1998, 62:269–277
48. Messiaen L, Callens T, De Paepe A, Craen M, Mortier G: Characterisation of two different nonsense mutations, C6792A and C6792G, causing skipping of exon 37 in the NF1 gene. Hum Genet 1997, 101:75–80
49. Wittchen ES, Haskins J, Stevenson BR: Protein interactions at the tight junction: actin has multiple binding partners, and ZO-1 forms independent complexes with ZO-2 and ZO-3. J Biol Chem 1999, 274: 35179–35185
50. Hirano A, Matsui T: Vascular structures in brain tumors. Hum Pathol 1975, 6:611–621
51. Dinda AK, Sarkar C, Roy S, Kharbanda K, Mathur M, Khosla AK, Banerji AK: A transmission and scanning electron microscopic study of tumoral and peritumoral microblood vessels in human gliomas. J Neurooncol 1993, 16:149–158
52. Bertossi M, Virgintino D, Maiorano E, Occhiogrosso M, Roncali L: Ultrastructural and morphometric investigation of human brain capillaries in normal and peritumoral tissues. Ultrastruct Pathol 1997, 21:41–49
53. Furuse M, Hirase T, Itoh M, Nagafuchi A, Yonemura S, Tsukita S: Occludin: a novel integral membrane protein localizing at tight junctions. J Cell Biol 1993, 123:1777–1788
54. Vorbrodt AW, Dobrogowska DH: Molecular anatomy of intercellular junctions in brain endothelial and epithelial barriers: electron microscopist's view. Brain Res Brain Res Rev 2003, 42:221–242